Multiscale Ordinal Symbolic Analysis of the Lang-Kobayashi Model for External-Cavity Semiconductor Lasers

Nianqiang Li, Luciano Zunino, A. Locquet, Byungchil Kim, Daeyoung Choi, Wei Pan, David Citrin

Multiscale ordinal symbolic analysis of the Lang-Kobayashi model for external-cavity semiconductor lasers

N. Li,[1] L. Zunino,[2,3,*] A. Locquet,[4,5,†] B. Kim,[4,5] D. Choi,[4,5] W. Pan,[1] and D. S. Citrin[4,5]

[1] *Center for Information Photonics and Communications, Southwest Jiaotong University, Chengdu, 610031 China*
[2] *Centro de Investigaciones Ópticas (CONICET La Plata - CIC), C.C. 3, 1897 Gonnet, Argentina*
[3] *Departamento de Ciencias Básicas, Facultad de Ingeniería, Universidad Nacional de La Plata, 1900 La Plata, Argentina*
[4] *School of Electrical and Computer Engineering, Georgia Institute of Technology, Atlanta, Georgia 30332-0250 USA*
[5] *UMI 2958 Georgia Tech-CNRS, Georgia Tech Lorraine, 2 Rue Marconi F-57070, Metz, France*
*Corresponding author: * lucianoz@ciop.unlp.edu.ar; † alexandre@gatech.edu*

Compiled February 8, 2015

We study experimentally and theoretically the permutation entropy (PE) of the optical intensity $I(t)$ of an external-cavity semiconductor DFB laser in the coherence collapse regime. Our PE analysis allows us to uncover the intrinsic dynamical complexity at *multiple timescales* of the delayed-feedback system, as well as to investigate how the experimental observations can be determined by modeling. An overall good agreement between experiment and theory corroborates the effectiveness of the Lang-Kobayashi model, though the model underestimates the entropy on the timescale of the relaxation oscillations and can lead to a time-delay signature that is less evident than in experiment, indicating a potential vulnerability of chaos encryption.

OCIS codes: (140.2020) Diode lasers; (140.5960) Semiconductor lasers; (190.3100) Instabilities and chaos.

Photonic systems exhibit ultrafast chaos as well a rich variety of other dynamical behaviors. Our focus is on external-cavity semiconductor lasers (ECLs) for which there are many applications [1–4]. Characterizing this behavior, coupled with the comparison to models, is a formidable problem since for a chaotic system, one cannot expect exact correspondence between experiment and theory. Here, we study experimentally and theoretically the permutation entropy (PE) [5] of the time-dependent intensity $I(t)$. Our comprehensive PE analysis allows us to uncover the intrinsic dynamical complexity at *multiple timescales* of the delayed-feedback system, as well as to investigate how experiment can be matched to the Lang-Kobayashi (LK) equations [6].

Matching experiment with the predictions of the LK model faces hurdles, such as band-limited detection, noise, and limited parameter control. In addition, entropies, Lyapunov exponents, and correlation dimensions, that are frequently used to characterize time-series complexity and can provide useful insights into the nature of nonlinear systems, are difficult to obtain experimentally in high-dimensional systems such as ECLs [7]. Up to now there has been a dearth of systematic studies to confirm the degree to which the LK model provides adequate understanding of actual ECLs.

There are a number of ways one might carry out such a program. One is to focus on low-order statistics extracted from $I(t)$, such as autocovariance (ACV) and probability density function (PDF). Recently, we found substantial agreement between theory and experiment for the ACVs with some discrepancies for the PDFs [8]. Another approach focuses on analyzing a measure of entropy, such as the Kolmogorov-Sinai (KS) entropy or the metric entropy [9]. Entropies indicate the degree to which future behavior of a time series (TS) can be predicted from its past history, and as such constitute important measures of dynamical complexity. Moreover, entropies can be used to analyze the dynamics over multiple timescales and may contain statistical information over many moments. Shannon entropy (ShE) has been shown rigorously to set a bound to the maximum rate of information-theoretic randomness extractible from $I(t)$. The KS entropy can be thought of measuring the time rate of creation of information as a chaotic orbit evolves and is related to the spectrum of Lyapunov exponents through Pesin's identity [9]. Computing such entropies from $I(t)$, however, has its own difficulties that frequently render such an attempt impractical.

PE [5, 10] is relatively simple to compute and serves as a surrogate for ShE obtained from the PDF by using the Bandt and Pompe recipe. PE quantifies complexity based on ordinal patterns in TS. Previously, some of us [11] showed numerically that PE evaluated at specific timescales for ECLs can recover important features characterized by KS entropy and thus provides valuable information about the complexity of chaotic lasers. Also for an ECL, Toomey and Kane [12] conducted an experimental study that further confirms the strong dependence of complexity on the timescale used in the PE calculation and found that evaluating the complexity with a PE delay equal to the external-cavity round-trip time τ_S produces results consistent with the notion of weak/strong chaos. Still, a comprehensive picture that reconciles experiment and theory across a range of parameters remains unavailable.

In this Letter, we analyze the LK model in a global way based on a multiscale ordinal symbolic analysis. Taking the characteristic time constants in the ECL into

consideration, the PE of $I(t)$ is calculated at various timescales over a range of feedback levels (theory, γ; experiment, η) and injection currents J on the basis of both numerical and experimental TS.

The setup consists of an intrinsically single-longitudinal-mode MQW InGaAsP DFB laser, at near 1550 nm wavelength with maximum cw power of 15 mW [8]. The free-running laser threshold current J_{th} is $\sim$9.27 mA. The position of a mirror determines $\tau_S = 2L/c$ (L=external-cavity length, c=speed of light) with L=65 cm giving $\tau_S = 4.3$ ns; the dimensionless experimental feedback rate η is controlled as described in [8]; when $\eta = 1$, $\sim 20\%$ of the optical power is fed back onto the laser diode (LD). J is held well above J_{th} of the solitary LD throughout the experiment. A fast photodiode with 12-GHz bandwidth is used to convert $I(t)$ to an electrical signal. A 12-GHz bandwidth, 40-GS/s real-time oscilloscope is employed to capture $I(t)$ for analysis.

To make a detailed comparison between experiment and theory, the LK model is used [6]; with $E(t)$ the complex electric field and $N(t)$ the carrier number, we have

$$\dot{E}(t) = \frac{(1+i\alpha)}{2}\left[G(t) - \frac{1}{\tau_p}\right]E(t) + \gamma E\left(t-\tau_S\right)e^{-i\Phi}, \tag{1}$$

$$\dot{N}(t) = \frac{J}{e} - \frac{N\left(t\right)}{\tau_N} - G(t)\left|E(t)\right|^2, \tag{2}$$

with $G(t) = g[N(t) - N_0]$ =optical gain (g =differential gain coefficient), N_0 = carrier density at transparency, α =linewidth-enhancement factor, Φ =optical feedback phase, τ_p =photon lifetime, τ_N =carrier lifetime, and $J = qJ_{th}$ (q=injection factor). The best agreement with the observed dynamics is for α=3, τ_p=2.65 ps, τ_N=2.5 ns, $g = 2.5 \times 10^{-8}$ ps^{-1}, and $N_0 = 1.3 \times 10^8$, $\Phi = 0$, giving $J_{th} \approx 9.27$ mA. Moderate noise (not included) does not significantly change the theoretical dynamics for the values of J considered [8]. In our previous work [8], we estimated a maximum theoretical feedback rate γ=25 ns^{-1}, corresponding to η=1 in our setup. Simulations were conducted with a fourth-order Runge-Kutta method with random initial conditions. To mimic filtering due to the detection of the amplified photodetector and oscilloscope, the theoretical TSs were filtered using a cascade of third- and ninth-order Butterworth filters with 12-GHz bandwidths [8]. This specific filtering processing helps us achieve very good qualitative agreement between numerics and experiments.

The experimental and theoretical TSs were analyzed through a multiscale ordinal symbolic approach, with PE computed based on a PDF constructed from $I(t)$ following Bandt and Pompe [5]. We took partitions given by comparison of neighboring values of the TSs, rather than partitioning the amplitude into different levels, which avoids amplitude threshold sensitivity and thus overcomes the misplacement problem of the partition [5]. This symbolic transformation keeps the information about the correlations present in $I(t)$, but neglects the

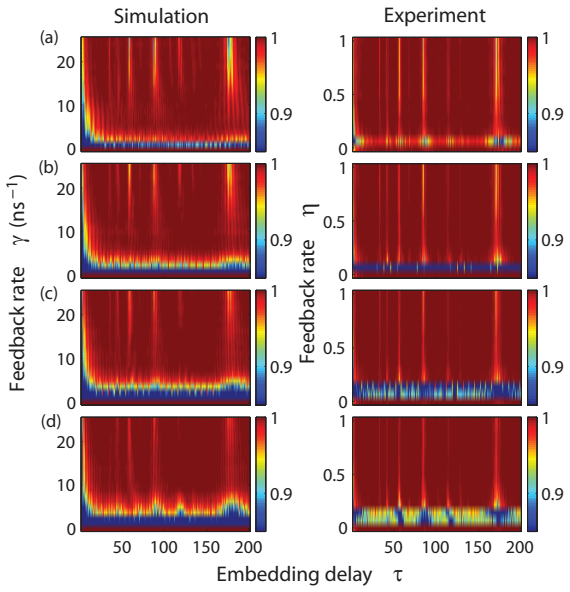

Fig. 1. PE estimated with D=6 as a function of τ and γ (η) for (a) q=1.4, (b) 1.7, (c) 2.0, and (d) 2.4.

information associated with the exact amplitude variations [13]. That is, a reasonable PDF of the generated ordinal patterns for a given TS can be obtained when two key embedding parameters related to the PE, *i.e.*, an ordinal pattern length D and an embedding delay τ, are appropriately chosen. Here, D and τ determine the number of symbols that forms the ordinal pattern, and the separation between consecutive symbols in each ordinal pattern, respectively. Moreover, it is well accepted that the TS length M should satisfy the condition $M \gg D!$ to obtain reliable statistics [5]. Thus, we analyzed time traces of $M = 4\times10^4$ samples separated by 25 ps (sampling period Ω_S=25 ps), and used values of D between 3 and 6, in both numerical simulations and experiments. It is worth noting that, if $M \gg D!$, more information can be obtained by estimating the PE with the largest D considered. Therefore, our results presented here are obtained for D=6, despite the fact that we have obtained equivalent experimental and simulation comparisons for other values of D (not shown). Moreover, it is important to note that by changing τ different timescales of the system are characterized ($\Omega_\tau = \tau\Omega_S$ with Ω_τ the timescale at which the analysis is being done).

Figure 1 shows typical examples of PE versus τ and γ (η) for four values of q, from model and experiment. It is well-established that PE exhibits pronounced local minima when τ matches harmonics and subharmonics of $\tau_S^* = \tau_S/\Omega_S = 172$ [10]. Indeed, this property has been proposed for time-delay identification [14]. As can be seen in Fig. 1, for $\eta\sim0$, PE in experiment is very high since the ECL is operating in a cw state and the recorded TSs are dominated by spontaneous emission (SE) and shot noise from the LD as well as noise in the photodiode and oscilloscope. Even though we did not consider

the influence of SE noise, qualitatively similar results are found for these low values of γ ($\sim$0). This is because the combined effect of numerical integration noise and of filtering leads to a noisy dynamics characterized by a PE near one. When γ (η) is slightly increased, the estimated PE in theory (experiment) is extremely small. We interpret this as follows: for such feedback levels, the chaos is not reached or well developed, so the ECL exhibits non-chaotic behaviors (periodic, quasi-periodic, intermittency); also, no fingerprint of τ_S is revealed because of the weakness of the external-cavity driving force F denoted as the feedback term in (1).

If γ (η) is further increased, F becomes dominant, many external-cavity modes participate simultaneously to the dynamics [15], and the laser exhibits fully-developed coherence collapse (CC) around these modes in our calculations and experiment. Interestingly, for higher γ (η), at all q shown, the drops in the calculated PE occur for τ matching τ_S^*, $\tau_S^*/2$, $\tau_S^*/3$, ..., and $\tau_S^*/(D-1)$ in both cases, which represents a common phenomenon in the dynamics of delayed-feedback systems indicating a deterministic link between samples separated by τ_S. Also, additional extrema at $\tau_S^*+\tau_{RO}/2$ (τ_{RO} =relaxation oscillation time, in the range between $\sim$ 0.1 and $\sim$ 0.2 ns) lead to a wider drop band $\sim\tau_S^*$ when compared to those of other delays [10, 12]. Figure 1 shows that numerical results are overall in good agreement with experimental observations.

We next show how the match between numerical and experimental PE varies with timescale chosen, revealing the intrinsic multiple-timescale features of the ECL. A short timescale ($\sim\tau_{RO}/2$) and two longer timescales ($\sim$ τ_S and one of its subharmonics) are considered.

Figures 2 (a)-(d) show PE as a function of γ (η) for various q, when evaluated at a short timescale of $\tau = 3$ (three times the sampling period, 75 ps). Note that such τ corresponds with a sufficiently high sample rate and helps us capture the dynamics at the fastest relevant timescale. Numerics and experiments show similar variations of PE versus γ (η). Quantitative discrepancies between numerics and experiments are noticed, as the simulated PE is typically smaller than its experimental counterpart, both for small and large γ (η). We checked that the addition of Langevin sources in the LK model to simulate SE noise does not influence significantly this discrepancy. Our comparative PE analysis thus reveals that the LK model does not reproduce perfectly the deterministic evolution of an ECL on short timescales corresponding to a fraction of $\tau_{\rm RO}$. Interestingly, this was not revealed by the (linear) ACV analysis we performed in [8] since the decorrelation time was shown to be well matched in simulation and experiments. Figures 2 (e)-(l) show typical examples of PE at long timescales from the LK model and experiment. Such choices of τ allow us to access information about complexity on these longer timescales. Interestingly, in Figs. 2 (e)-(l), there is a much better agreement between simulations and experiments, both in terms of curve shape and its absolute amplitude variation. Except for weakly developed dynamics resulting from a small γ (η), the numerical and experimental PE values are well matched. This indicates that LK correctly models statistical links on large timescales and in particular on the timescale of τ_S. There is a special case, though, for $q = 1.4$ and $\tau = 172$ [Fig. 2(i)], for which we find a counterintuitive result since PE for the noiseless LK model is slightly larger than for experiment [see the enlargement in Fig. 2(i)]. However, if a slightly larger embedding delay ($\tau > 172$) is chosen for the numerical analysis for this q, one finds much smaller PE in numerics than experiment, consistent with a lower degree of randomness in the stronger pulsing dynamics generated by LK at q=1.4 compared to experiment [8]. This means that uncertain calibration of τ between numerics and experiment, due to the difficult-to-determine influence of the response time [14], may help to interpret the surprising phenomenon in Fig. 2(i).

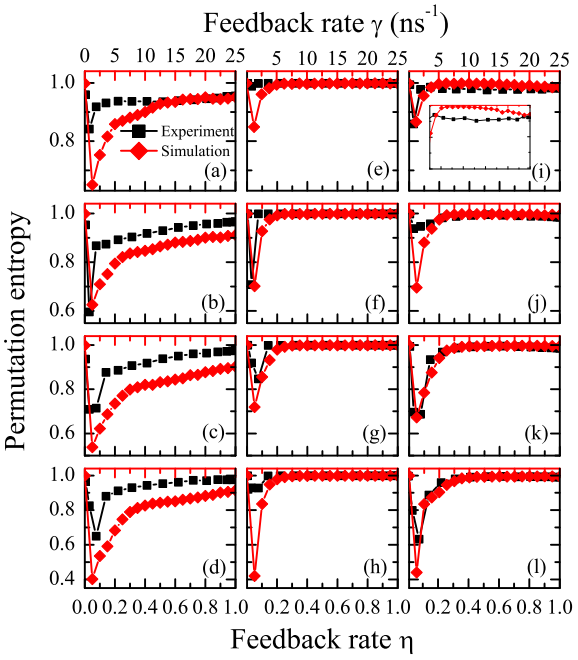

Fig. 2. PE estimated with $D = 6$ as a function of γ (η) for (a, e, i) $q = 1.4$, (b, f, j) 1.7, (c, g, k) 2.0, and (d, h, l) 2.4. Left: $\tau = 3$ (75 ps); middle: $\tau = 50$ (1.25 ns); right: $\tau = 172$ (4.3 ns). Squares: experiment; diamonds: numerics. The inset is an enlargement of Fig. 2(i).

It should be noted that a local minimum of PE is expected for τ_S and its harmonics and subharmonics [14]. Looking more carefully at the two-dimensional plots of PE in Fig. 1, one sees that τ_S is not well detected in numerics, for a particular range of γ, *i.e.*, when γ takes values between $\sim$ 5 and $\sim$ 15 ns^{-1}. In contrast, more pronounced drops are seen at intermediate γ (η) in experiment. This behavior holds for the four values of q chosen. According to our finding, in numerics τ_S seems to be well suppressed or even hidden, whereas the experimental analysis clearly shows its presence. The identifi-

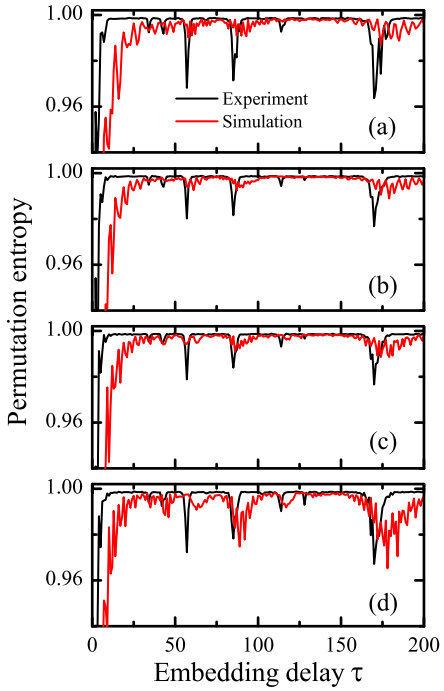

Fig. 3. PE estimated with $D = 6$ as a function of τ for (a) $q = 1.4$, (b) 1.7, (c) 2.0, and (d) 2.4, where $\gamma = 8$ ns^{-1} and $\eta = 0.31$. Black: experiments; red: numerics.

cation of τ_S has attracted intensive research interest in recent years ([10,14,16–19] and references therein), most of which drew conclusions only based on numerical simulations or on poorly matched model and experimental data. Thus, erroneous conclusions about the success for concealing τ_S may be derived from an exclusive numerical study. Also, we observe the presence of a shift in the delay of the system in numerics, as shown in Fig. 3 for an intermediate γ (η). As is seen, the minimum of PE for the numerical analysis is located at a slightly larger $\tau \approx 175$ than expected (172). We also confirm such shift by carrying out the ACV analysis (not shown).

Finally, we would like to discuss the origin of the discrepancy between model and experiment at short timescales. The good matching of PE at the timescale of the delay can lead one to consider that the effect of delayed optical feedback in the laser cavity is properly taken into account in LK [6]. The discrepancy, which is present only for small τ, probably originates in the imperfect modeling of the inner laser dynamics. In particular, the modeling of gain saturation, SE noise, and spatial effects may be required to achieve a better fit.

In conclusion, we have reported on a yet unexplored comparison of ECL dynamics with the LK model under the lens of a PE analysis. High resolution maps of PE of $I(t)$ generated by an ECL in the fully developed CC regime, comparing experimental measurements with the LK model calculations, as functions of γ (η) and τ have been obtained. We find that numerics are in overall agreement with experiment despite the presence of some discrepancies. Specifically, the ECL under study seems to generate more entropy on short timescales (fractions of τ_{RO}) than the LK model predicts, while PE values are in very good agreement on longer timescales, and in particular on the timescale of τ_S, indicating a good modeling in LK, from a statistical point of view, of the effect of the delayed optical feedback. Therefore, it appears that modeling efforts should focus on better reproducing the fast dynamics resulting from an excitation of the relaxation oscillations between photon and carrier populations in a DFB laser. Moreover, we have found that signatures of τ_S may be more evident in the PE obtained from experiment than numerics, indicating a vulnerability of chaos-encrypted communication systems [19].

References

1. A. Argyris, D. Syvridis, L. Larger, V. Annovazzi-Lodi, P. Colet, I. Fischer, J. Garcia-Ojalvo, C. R. Mirasso, L. Pesquera, and K. A. Shore, Nature **438,** 343 (2005).
2. F. Y. Lin and J. M. Liu, IEEE J. Sel. Top. Quantum Electron. **10,** 991 (2004)
3. A. Uchida, K. Amano, M. Inoue, K. Hirano, S. Naito, H. Someya, I. Oowada, T. Kurashige, M. Shiki, S. Yoshimori, K. Yoshimura, and P. Davis, Nat. Photonics. **2,** 728 (2008).
4. L. Appeltant, M. C. Soriano, G. Van der Sande, J. Danckaert, S. Massar, J. Dambre, B. Schrauwen, C. R. Mirasso, and I. Fischer, Nat. Commun. 2, 468 (2011).
5. C. Bandt and B. Pompe, Phys. Rev. Lett. **88,** 174102 (2002).
6. R. Lang and K. Kobayashi, IEEE J. Quantum Electron. **16,** 347 (1980).
7. J. P. Eckmann and D. Ruelle, Rev. Mod. Phys. **57,** 617 (1985).
8. N. Li, B. Kim, A. Locquet, D. Choi, W. Pan, and D. S. Citrin, Opt. Lett. **39,** 5949 (2014).
9. E. Ott, *Chaos in dynamical systems* (Cambridge university press, 2002).
10. M. C. Soriano, L. Zunino, O. A. Rosso, I. Fischer, and C. R. Mirasso, IEEE J. Quantum Electron. **47,** 252 (2011).
11. L. Zunino, O. A. Rosso, and M. C. Soriano, IEEE J. Sel. Top. Quantum Electron. **17,** 1250 (2011).
12. J. P. Toomey and D. M. Kane, Opt. Express **22,** 1713 (2014).
13. A. Aragoneses, N. Rubido, J. Tiana-Alsina, M. C. Torrent, and C. Masoller, Sci. Rep. **3,** 1778 (2013).
14. L. Zunino, M. C. Soriano, I. Fischer, O. A. Rosso, and C. R. Mirasso, Phys. Rev. E **82,** 046212 (2010).
15. C. Masoller and N. B. Abraham, Phys. Rev. A **57,** 1313 (1998).
16. D. Rontani, A. Locquet, M. Sciamanna, and D. S. Citrin, Opt. Lett. **32,** 2960 (2007).
17. J. Wu, G. Xia, and Z. Wu, Opt. Express **17,** 20124 (2009).
18. S. Priyadarshi, Y. Hong, I. Pierce, and K. A. Shore, IEEE J. Sel. Top. Quantum Electron. **19,** 1700707 (2013).
19. R. M. Nguimdo, P. Colet, L. Larger, and L. Pesquera, Phys. Rev. Lett. **107,** 034103 (2011).

References

1. A. Argyris, D. Syvridis, L. Larger, V. Annovazzi-Lodi, P. Colet, I. Fischer, J. Garcia-Ojalvo, C. R. Mirasso, L. Pesquera, and K. A. Shore, "Chaos-based communications at high bit rates using commercial fibre-optic links," Nature **438,** 343 (2005).
2. F. Y. Lin and J. M. Liu, "Chaotic lidar," IEEE J. Sel. Top. Quantum Electron. **10,** 991 (2004)
3. A. Uchida, K. Amano, M. Inoue, K. Hirano, S. Naito, H. Someya, I. Oowada, T. Kurashige, M. Shiki, S. Yoshimori, K. Yoshimura, and P. Davis, "Fast physical random bit generation with chaotic semiconductor lasers," Nat. Photonics. **2,** 728 (2008).
4. L. Appeltant, M. C. Soriano, G. Van der Sande, J. Danckaert, S. Massar, J. Dambre, B. Schrauwen, C. R. Mirasso, and I. Fischer, "Information processing using a single dynamical node as complex system," Nat. Commun. 2, 468 (2011).
5. C. Bandt and B. Pompe, "Permutation entropy: a natural complexity measure for time series," Phys. Rev. Lett. **88,** 174102 (2002).
6. R. Lang and K. Kobayashi, "External optical feedback effects on semiconductor injection laser properties," IEEE J. Quantum Electron. **16,** 347 (1980).
7. J. P. Eckmann and D. Ruelle, "Ergodic theory of chaos and strange attractors," Rev. Mod. Phys. **57,** 617 (1985).
8. N. Li, B. Kim, A. Locquet, D. Choi, W. Pan, and D. S. Citrin, "Statistics of the optical intensity of a chaotic external-cavity DFB laser," Opt. Lett. **39,** 5949 (2014).
9. E. Ott, *Chaos in dynamical systems* (Cambridge university press, 2002).
10. M. C. Soriano, L. Zunino, O. A. Rosso, I. Fischer, and C. R. Mirasso, "Time scales of a chaotic semiconductor laser with optical feedback under the lens of a permutation information analysis," IEEE J. Quantum Electron. **47,** 252 (2011).
11. L. Zunino, O. A. Rosso, and M. C. Soriano, "Characterizing the hyperchaotic dynamics of a semiconductor laser subject to optical feedback via permutation entropy," IEEE J. Sel. Top. Quantum Electron. **17,** 1250 (2011).
12. J. P. Toomey and D. M. Kane, "Mapping the dynamic complexity of a semiconductor laser with optical feedback using permutation entropy," Opt. Express **22,** 1713 (2014).
13. A. Aragoneses, N. Rubido, J. Tiana-Alsina, M. C. Torrent, and C. Masoller, "Distinguishing signatures of determinism and stochasticity in spiking complex systems," Sci. Rep. **3,** 1778 (2013).
14. L. Zunino, M. C. Soriano, I. Fischer, O. A. Rosso, and C. R. Mirasso, "Permutation-infromation-theory approach to unveil delay dynamics from time-series analysis," Phys. Rev. E **82,** 046212 (2010).
15. C. Masoller and N. B. Abraham, "Stability and dynamical properties of the coexisting attractors of an external-cavity semiconductor laer," Phys. Rev. A **57,** 1313 (1998).
16. D. Rontani, A. Locquet, M. Sciamanna, and D. S. Citrin, "Loss of time-delay signature in the chaotic output of a semiconductor laser with optical feedback," Opt. Lett. **32,** 2960 (2007).
17. J. Wu, G. Xia, and Z. Wu, "Suppression of time delay signatures of chaotic output in a semiconductor laser with double optical feedback," Opt. Express **17,** 20124 (2009).
18. S. Priyadarshi, Y. Hong, I. Pierce, and K. A. Shore, "Experimental investigations of time-delay signature concealment in chaotic external cavity VCSELs subject to variable optical polarization angle of feedback," IEEE J. Sel. Top. Quantum Electron. **19,** 1700707 (2013).
19. R. M. Nguimdo, P. Colet, L. Larger, and L. Pesquera, "Digital key for chaos communication performing time delay concealment," Phys. Rev. Lett. **107,** 034103 (2011).